Cosmological probes of grand unification: Primordial black holes and scalar-induced gravitational waves

Anish Ghoshal,[1,*] Ahmad Moursy,[2,†] and Qaisar Shafi[3,‡]

[1]*Institute of Theoretical Physics, Faculty of Physics, University of Warsaw, ul. Pasteura 5, 02-093 Warsaw, Poland*

[2]*Department of Basic Sciences, Faculty of Computers and Artificial Intelligence, Cairo University, Giza 12613, Egypt*

[3]*Bartol Research Institute, Department of Physics and Astronomy, University of Delaware, Newark, Delaware 19716, USA*

(Received 24 June 2023; accepted 6 September 2023; published 29 September 2023)

We investigate the inflationary cosmology involving an $SU(5)$ GUT (grand unified theory) singlet scalar with nonminimal coupling to the Ricci scalar. In this scenario the scale of grand unification is set by the inflaton vacuum expectation value when the inflaton rolls down its potential towards its minimum v, thereby relating inflationary dynamics to GUT symmetry breaking with a prediction of $r \simeq 0.025$ for the tensor-to-scalar ratio to be tested by the next generation of CMB experiments. We show in this inflationary framework involving an inflection point how a suitable choice of parameters in $SU(5)$ leads to a bump in the scalar power spectrum with the production of primordial blackholes (PBH) of masses 10^{17}–10^{18} g (10^{-16}–$10^{-15} M_\odot$). We derive the constraints on the self-quartic and mixed-quartic couplings of the inflaton in $SU(5)$ that are consistent with the inflationary analysis. Moreover, we also show that this scenario leads to large amplitude induced second-order tensor perturbations propagating as gravitational waves (GWs) with an amplitude $\Omega_{\rm GW}h^2 \sim 5 \times 10^{-10}$–$10^{-8}$ and peak frequency $f_{\rm peak} \sim (0.1\text{–}300)$ Hz, which can be detected in the next-generation GW observatories like LISA, BBO, ET, etc. Thus, we unify the $SU(5)$ framework with PBH via inflection-point inflation showing how the upcoming measurements of PBH and GW will enable us to probe the scale of $SU(5)$ symmetry breaking, and thereby complementing the laboratory-based experiments. We also discuss scenarios involving the Pati-Salam and trinification gauge groups and its impact on quartic and mixed-quartic couplings that may lead to PBH and detectable GW signals.

DOI: 10.1103/PhysRevD.108.055039

I. INTRODUCTION

One of the most striking predictions of grand unified theories (GUTs) is proton decay [1–7], and Super-Kamiokande has set stringent constraints on the typical decay channels such as $p \to \pi^0 e^+$, $K^+\bar{\nu}$ with the proton lifetime exceeding 10^{34} years [8,9]. This approximately translates into a bound on the GUT symmetry-breaking scale to be $M_{\rm GUT}$ to be $> 5 \times 10^{15}$ GeV. There are even more very exciting prospects ongoing and during the current decade, thanks to the upcoming large-scale and large-volume neutrino detectors, namely experiments like DUNE [10], Hyper-Kamiokande [11], and JUNO [12], which promise to improve the lower bound on $M_{\rm GUT}$ by an order of magnitude or so, or even more excitingly possibly detect proton decay.

Besides the motivations of UV completion (where all the SM gauge couplings are unified) GUTs also formed the basis of the first proposal for cosmic inflation, an accelerated expansion of the early Universe, which essentially resolves the horizon and the flatness problems of big bang cosmology, as well as provide the initial seed of density fluctuations that grow into the inhomogeneous Universe that we observe today [13–16].[1] Such inflation driven by GUTs turned out to be unsuccessful due to measurements of the CMB, however the quantum generation of the primordial fluctuations seeding the large-scale structure (LSS) of the Universe was a successful scenario. Whether

*anish.ghoshal@fuw.edu.pl
†a.moursy@fci-cu.edu.eg
‡qshafi@udel.edu

[1]Later on, inflation was studied in the context of gravity effective theories like the Starobinsky scenario [17,18].

or not the origin of inflationary cosmology is from particle physics, the rapidly increasing data from cosmological precision measurements, particle-physics experiments and astrophysical observations lead us to the quest to find a coherent picture of the early Universe based on particle physics to begin with. Inflationary studies based on conformal GUT theories employed the Coleman-Weinberg potential for a GUT singlet-scalar inflaton field with minimal coupling to gravity [19,20]. It was soon followed by studies of GUT models containing topologically stable cosmic strings [21,22] and intermediate scale monopoles [23–27], and in GUT models such as $SO(10)$ these may survive an inflationary epoch. Later on, GUT models involving dark sector physics were also considered [28–30].

Going beyond the minimal coupling to gravity, the Standard Model (SM) Higgs inflation and scalar fields with nonminimal coupling to gravity (the Ricci scalar) [31] provide naturally flat inflaton potentials to scalar fields in general [32–39] that may drive inflation with predictions of spectral indices that are compatible with the current CMB measurements. In some models there appear certain characteristic features in the potential which may lead to production of huge scalar fluctuations that may seed formation of primordial black holes (PBHs) [40] when length scales around the critical point reenter the Hubble horizon after inflation has ended. Moreover, such PBHs may even constitute part or all of the dark matter (DM) in the Universe [41–54], thus providing a novel DM candidate.[2] Moreover, the recent detection of gravitational waves from black hole mergers by LIGO and Virgo [56] has ushered in a new age in GW astronomy of the study of PBHs [57,58], with several proposed models of inflation involving scalar fields [59–66] that could produce PBH dark matter in a mass range observable by current, or in upcoming, gravitational wave experiments.[3] These predictions are, of course, subject to the stringent constraints such as lensing and gamma-ray bursts and other astrophysical measurements at our disposal [77–79]. Only few regions remain in the spectrum of PBH mass that still allow a sizeable PBH population. These are basically two narrow mass windows at 10^{18} g and 4×10^{19} g, and a PBH mass window around $10^{34} \ldots 10^{35}$ g $\approx 25 \ldots 100 M_{\odot}$ which is very near to the LIGO/Virgo range that may allow for PBHs to be DM. All initial PBH masses $M_{\rm PBH} < 10^{9}$ g are however disallowed as they correspond to PBHs that evaporate before big bang nucleosynthesis (BBN) down to Planck scale relics without spoiling the baryon asymmetry [77,79].

In addition to having PBH formation, second-order tensor perturbations may be generated from the enhancement of the scalar curvature perturbations. This has been investigated in recent works, which lead to detectable GW signals in the upcoming GW detectors [64,80–94].

With the scale of GUT physics largely out of reach of laboratory experimental facilities, in this paper we propose a $SU(5)$ inflationary scenario which leads to large scalar perturbations and formation of PBHs as the entirety of DM in the Universe, and show how the GUT scale can be probed in the induced GW predictions with the upcoming GW experiments. The scenario is consistent with the lower bound on $M_{\rm GUT}$ experiments, proton decay, as well as theoretical constraints on the GUT parameter space arising from quantum corrections and the demand of unification of the SM gauge couplings. We show that the scale of grand unification can be probed by cosmological observables including spectral distortions, PBH and GW predictions, and in future may lead to novel constraints that may pin down the GUT scale. Our discussion also extends to other unified models based on gauge groups $SU(4)_C \times SU(2)_L \times SU(2)_R$ [95] and $SU(3)_C \times SU(3)_L \times SU(3)_R$ [96–98], in which case $M_{\rm GUT}$ can be lower than the standard scale of 5×10^{15}–10^{16} GeV.

The paper is organized as follows. In Sec. II, we discuss the model of inflation, and in Sec. III we discuss the GUT symmetry breaking and the relation with inflationary parameters. In Sec. IV, we describe the scalar perturbations and the solution to the Mukhanov-Sasaki equations resulting in the spike in the power spectrum. This leads to induced GWs and the production of PBHs as DM which we discuss in Sec. V. Finally, we end with some discussion and outlook in Sec. VI.

II. AN INFLATION MODEL WITH INFLECTION POINT

We consider an inflaton ϕ which is a GUT singlet and nonminimally coupled to gravity. The action in Jordan frame is given by

$$S_J = \int d^4x\sqrt{-g}\left[\frac{1}{2}f(\phi)R - \frac{1}{2}g^{\mu\nu}\partial_\mu\phi\partial_\nu\phi - V_J(\phi)\right], \quad (1)$$

with $V_J(\phi)$ being the scalar potential that has the most general form of a renormalizable potential, with nonzero vacuum expectation value (VEV) of ϕ,

$$V_J(\phi) = \frac{1}{2}m^2(\phi - v)^2 - \frac{1}{3}\alpha\mu(\phi - v)^3 + \frac{1}{4}\lambda(\phi - v)^4, \quad (2)$$

and the nonminimal coupling to gravity is given by [31]

$$f(\phi) = 1 + \xi\phi^2. \quad (3)$$

[2]SM Higgs Inflation may also lead to detectable scalar-induced GW signals, see Ref. [55].

[3]There is an ongoing debate regarding the formation of PBH as DM with discrepancies coming from one-loop effects in cosmological perturbation theory, see Refs. [67–76]. In this paper we do not go into details of such issues and instead discuss if GUT models may yield PBH (dark matter or some fraction thereof), and provide detectable GW signals as a novel probe of such unification.

Here α, λ, and ξ are dimensionless couplings, while m, μ are dimensionful mass scales. The global minimum is located at $\langle\phi\rangle = v$, at which the potential is zero. We work in Planck units, where the reduced Planck mass $M_{\rm Pl} = 2.43 \times 10^{18}$ GeV is set to unity. In the Einstein frame $g_E^{\mu\nu} = f(\phi) g^{\mu\nu}$, the action has the form

$$S_E = \int d^4x\sqrt{-g_E}\left[\frac{1}{2}R_E - \frac{1}{2}g_E^{\mu\nu}\partial_\mu\sigma\partial_\nu\sigma - V_E(\sigma(\phi))\right], \quad (4)$$

where the field σ, with canonical kinetic terms, is defined in terms of ϕ via

$$\left(\frac{d\sigma}{d\phi}\right)^2 = \frac{1}{f(\phi)} + \frac{3}{2}\left(\frac{f'(\phi)}{f(\phi)}\right)^2 = \frac{1+\xi(1+6\xi)\phi^2}{(1+\xi\phi^2)^2}, \quad (5)$$

and the inflationary potential V_E is given in terms of ϕ by

$$V_E(\phi) = \frac{V_J(\phi)}{f(\phi)^2} = \frac{\frac{1}{2}m^2(\phi-v)^2 - \frac{1}{3}\alpha\mu(\phi-v)^3 + \frac{1}{4}\lambda(\phi-v)^4}{(1+\xi\phi^2)^2}. \quad (6)$$

With the redefinitions, $x = (\phi - v)/\mu$, $m^2 = \lambda\mu^2$, $a = \alpha/\lambda$, and $b = \xi\mu^2$, the potential can be recast in the form

$$V(x) = \frac{\lambda v^4}{12}\frac{x^2(6-4ax+3x^2)}{\left[1+b\left(\frac{v}{\mu}+x\right)^2\right]^2}, \quad (7)$$

where we have dropped the subscript E, for simplicity. This potential features an asymptotically flat direction for very large x, which is suitable for driving inflation. For $x \gg 1$, $V \to V_0 = \frac{\lambda v^4}{4b}$.

A. Inflection points and ultraslow-roll regime

We are interested in inflection points of the potential (7), $V''(x) = 0$, around which the inflaton encounters ultraslow roll (USR) regime, and therefore we require that $V'(x) \approx 0$. We analyze the critical values of the potential (7) by solving the equation $V'(x) = 0$. One solution to the latter equation represents the true minimum at $x = 0$, and the others are solutions to the cubic equation

$$c_0 + c_1 x + c_2 x^2 + c_3 x^3 = 0, \quad (8)$$

with

$$c_0 = 1, \qquad c_1 = -a, \qquad c_2 = \frac{3\mu^2 + b(3v^2 - 2a\mu v - 3\mu^2)}{3(bv^2+\mu^2)}, \qquad c_3 = \frac{b\mu(a\mu+3v)}{3(bv^2+\mu^2)}. \quad (9)$$

Generally, there are three solutions, x_1 and $x_{2,3} = x_0 \pm iy_0$, with

$$x_1 = -\frac{c_2}{3c_3} - \frac{1}{3c_3}\left(\Theta(c_i) + \frac{D}{\Theta(c_i)}\right), \quad (10)$$

$$x_0 = -\frac{c_2}{3c_3} + \frac{1}{6c_3}\left(\Theta(c_i) + \frac{D}{\Theta(c_i)}\right), \quad (11)$$

$$y_0 = \frac{1}{2\sqrt{3}c_3}\left(\Theta(c_i) - \frac{D}{\Theta(c_i)}\right). \quad (12)$$

Here

$$\Theta(c_i)^3 = (C - \sqrt{C^2 - D^3}), \quad (13)$$

with $D = c_2^2 - 3c_1c_3 = c_2^2 + 3ac_3$ and $C = \frac{1}{2}(2c_2^3 - 9c_1c_3c_2 + 27c_0c_3^2)$. Clearly, $x_1 < 0$, and x_2, x_3 are real if, $\Theta = C^{1/3} = \sqrt{D}$. In this case, $x_2 = x_3 = x_0$ will be a simultaneous solution for $V''(x) = 0$ as well, namely,

$$x_0 = \frac{-c_2 + D^{1/2}}{3c_3}. \quad (14)$$

In the case of vanishing VEV, $v = 0$, and $c_0 = 1$, $c_1 = -a$, $c_2 = 1 - b$, $c_3 = \frac{ab}{3}$, the analysis of our potential reduces to the model described in Ref. [99].

The potential (7) has five independent parameters, namely, (λ, μ, a, b, v). However, the existence of an inflection point depends only on (a, b, μ, v). In particular, the desired inflection point exists at a critical value for $b = b_c(a, v)$, and hence the inflaton VEV v plays an important role in the dynamics around the inflection point. This is one of the main differences from [99], in which $v = 0$ and accordingly b_c is independent of v, μ

$$b_c(a) = 1 - \frac{1}{3}a^2 + \Delta(a), \qquad \Delta(a) = \frac{a^2}{3}\left(\frac{9}{2a^2} - 1\right)^{2/3}. \quad (15)$$

This case is illustrated by the black curve in Fig. 2. The other curves depict the change in b_c versus a for different values of nonzero v and different values of μ.

The nonzero VEV of ϕ will affect the slope and the curvature of the potential during inflation and around the inflection point, as illustrated in Fig. 1, where we have shown the effect of changing VEV v on the shape of the potential.

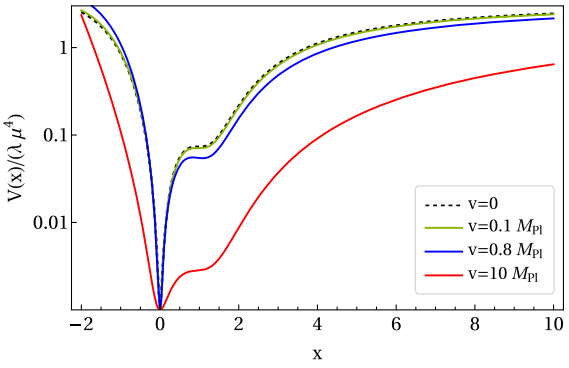

FIG. 1. Plot of the inflation potential (7) on y-axis versus the inflaton values x. Different colors correspond to different values of the VEV v.

B. Slow-roll approximation and dynamics around the inflection point

In the slow-roll approximation (SRA), the slow-roll parameter ϵ_V and η_V are given in terms of the potential as follows:

$$\epsilon_V = \frac{1}{2\mu^2}\left(\frac{V'(x)}{V(x)}\right)^2\left(\frac{d\sigma}{d\phi}\right)^{-2}, \tag{16}$$

$$\eta_V = \frac{1}{\mu^2}\left(\frac{V''(x)}{V(x)}\right)\left(\frac{d\sigma}{d\phi}\right)^{-2} - \frac{1}{\mu}\frac{V'(x)}{V(x)}\left(\frac{d\sigma}{d\phi}\right)^{-3}\frac{d^2\sigma}{d\phi^2}, \tag{17}$$

and the number of e-folds is given by

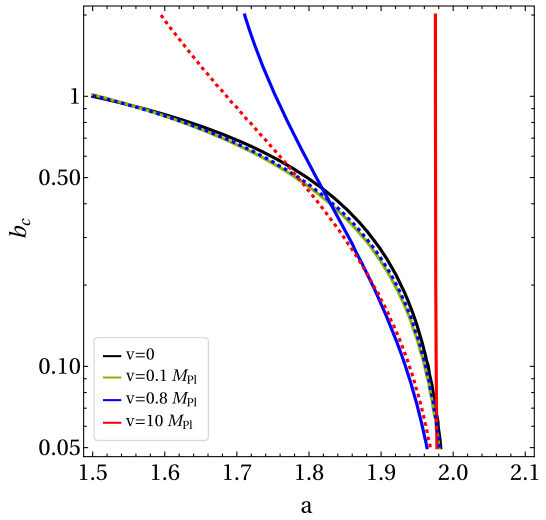

FIG. 2. The change of critical value b_c versus a, with different values of v represented by different colors. The solid curves correspond to $\mu^2 = 0.5$, dashed curves correspond to $\mu^2 = 0.01$, and dotted curves correspond to $\mu^2 = 5$.

$$N = \int_{x_e}^{x_*} \frac{1}{\sqrt{2\epsilon_V}}\frac{d\sigma}{d\phi}dx. \tag{18}$$

As indicated in Ref. [99], as the inflaton passes through the inflection point, the integrand in Eq. (18) diverges in the SRA. Therefore, we follow [99] by considering a near-inflection point, where $b = b_c(a,\mu,v) - \varepsilon$, with a resonance parameter $0 < \varepsilon \ll 1$. Accordingly, one can control the number of e-folds spent at $x = x_0$ by choosing appropriate values of ε, μ, and v. Hence, a significant peak in the power spectrum can be produced.

III. GAUGE SYMMETRY BREAKING

The part of the potential that dictates the interaction of the inflaton ϕ with some gauge symmetry-breaking scalar χ_D is given by

$$V_J(\phi,\chi_D) = -\frac{1}{2}\beta_D^2\phi^2\chi_D^2 + \frac{\lambda_D}{4}\chi_D^4, \tag{19}$$

where we consider, for simplicity, χ_D as a canonically normalized real scalar field in D-dimensional representation of the gauge group. This potential induces a vacuum expectation value for χ_D given by

$$\langle\chi_D\rangle = (\beta_D/\sqrt{\lambda_D})v \equiv M_{\rm SB}, \tag{20}$$

when the inflaton reaches its true minimum at v, and therefore,

$$\beta_D = \frac{\sqrt{\lambda_D}M_{\rm SB}}{v}. \tag{21}$$

In a GUT gauge group, such as $SU(5)$ gauge symmetry, the gauge coupling is order unity, with the structure constant given by $\alpha_{\rm GUT} = \frac{g_{\rm GUT}^2}{4\pi} \sim \frac{1}{50}$, with a typical GUT scale $M_{\rm GUT} \sim 5\times10^{15}$–$1\times10^{16}$ GeV. Accordingly, the contribution to the renormalization of the quartic coupling λ_D introduces a lower bound on the χ_D quartic coupling. For example, if we assume $\lambda_D \gtrsim 10^{-2}$, then this is translated to a lower bound on β_D, from Eq. (20)

$$\sqrt{4\pi} > \beta_D \gtrsim \frac{0.1M_{\rm SB}}{v}, \tag{22}$$

where the upper bound has been considered from the perturbativity conditions. Accordingly, a lower bound on the inflaton VEV is given by $v \gtrsim 2.05\times10^{-4}M_{\rm Pl}$.

In this regard, let us discuss the role of $SU(5)$ Higgs χ_D, during inflation, where the inflaton energy density during inflation is $\rho_\phi \sim V(\phi_*) \sim 10^{-9}M_{\rm Pl}^4$, and the inflation scale is given by

TABLE I. Three benchmark points for the model parameters used to generate the distributions presented in Figs. 4–6.

	$v(\mathrm{M_{Pl}})$	$\mu^2(\mathrm{M_{Pl}^2})$	a	b_c	ε	λ	λ_D	M_{SB} (GeV)
BP1	0.1	0.5	1.83457037	0.3895	3.24×10^{-2}	2.7×10^{-9}	10^{-4}	10^{15}
BP2	0.8	2	1.9090835	0.198991	10^{-7}	6.1×10^{-11}	10^{-3}	2×10^{15}
BP3	10	5	1.97677052	0.06562	10^{-6}	5.5×10^{-12} 4.1×10^{-12}	10^{-2}	6.8×10^{15}

TABLE II. CMB observables corresponding to BPs in Table I.

	n_s	r	A_s	N_{CMB}	ϕ_*
Ob(BP1)	0.9487	0.02518	2.2×10^{-9}	46.58	16.55
Ob(BP2)	0.953	0.0267	2.2×10^{-9}	59.4	30.77
Ob(BP3)	0.954 0.96	0.0758 0.064	2.2×10^{-9}	58 64	60 65.14

$$V^{1/4} = 10^{16}\left(\frac{r}{0.01}\right)\ \mathrm{GeV}. \tag{23}$$

According to the latest Planck and BICEP measurements on the upper bound on the tensor-to-scalar ratio (r), Planck 18 at 68% C.L. (0.1277 at 2σ) and at 95% C.L. (0.0684 at 1σ). While BICEP gives at 68% C.L. (0.0371 at 2σ) and at 95% C.L. (0.0257 at 1σ) [100,101]. We present the predictions of the tensor-to-scalar ratio values r in Table II, for the benchmark points (BPs) chosen in Table I. Likewise, the energy scale of inflation rages between 2.5×10^{16}–6.4×10^{16} GeV for our choices of the benchmark points. On the other hand, the value of the $SU(5)$ symmetry breaking scalar, during inflation, is $\chi_{D*} = \frac{\beta_D}{\sqrt{\lambda_D}}\phi_*$. Therefore, during inflation,

$$\rho_\chi \sim \frac{2\beta_D^4}{\lambda_D}\phi_*^4 = 2\lambda_D\left(\frac{M_{\mathrm{SB}}}{v}\right)^4\phi_*^4. \tag{24}$$

In this paper we are interested in the regions of parameter space where inflation is driven by ϕ only. In this case, energy density of ϕ will be dominant during inflation if $\rho_\chi < \rho_\phi$. In Fig. 3 we show the allowed regions under the curves in the $M_{\mathrm{SB}} - \lambda_D$ plane, for which the energy density of ϕ dominates the universe during inflation. The different curves correspond to different values of the inflaton VEV. The horizontal dashed black lines give different symmetry-breaking scales 5×10^{15} GeV and 7×10^{15} GeV, that are typical GUT scales where $SU(5)$ is broken. At these values, $\lambda_D \gtrsim 0.01$ for $v = 10M_{\mathrm{Pl}}$ which is consistent with Planck 2018 measurements, while a tuning is required to $\lambda_D \gtrsim 6 \times 10^{-5} - 2.5 \times 10^{-5}$ for $v = 0.8M_{\mathrm{Pl}}$, and $\lambda_D \gtrsim 2 \times 10^{-8} - 6.7 \times 10^{-8}$ for $v = 0.1M_{\mathrm{Pl}}$ in order to be consistent with BICEP measurements. As a matter of fact, the quartic coupling λ_D can be tuned $\lambda_D \sim 10^{-5}$ with an extended matter sector due to cancellations between gauge and Yukawa quantum corrections, if one considers an appropriate number of vectorlike fermions that couple to χ_D [102] which may lead to some fine-tuning. As shown in Fig. 3, such smaller quartic values allow for smaller inflaton VEV (v). Moreoever we have been focusing on the gauge group to be $SU(5)$ of GUT symmetry breaking scenario.

On the other hand, the horizontal dashed purple line corresponds to symmetry-breaking scale 2.4×10^{14} GeV that can be the scale of Pati-Salam unified theory with gauge symmetry $(SU(4) \times SU(2)_L \times SU(2)_R)^4$ or even trinification scenarios, with $\lambda_D \gtrsim 0.01$. The values of the symmetry-breaking parameters as well as the inflationary

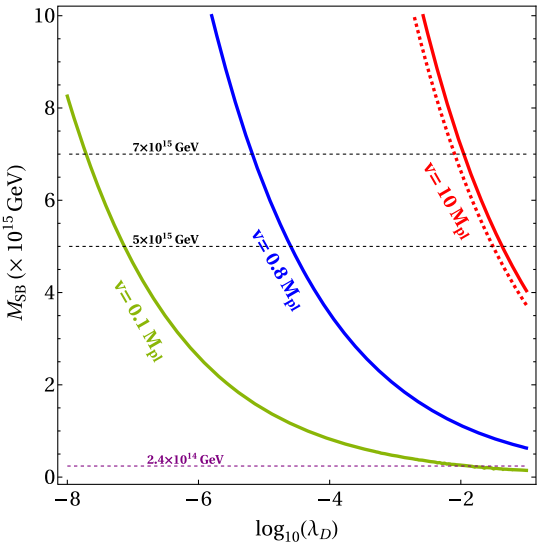

FIG. 3. Allowed regions (below the curves) in the $M_{SB} - \lambda_D$ plane, for different values of the inflaton VEV. The solid (dashed) red curves correspond to the same VEV, $v = 10\mathrm{M_{Pl}}$, but have different values of tensor to scalar ratio as shown in detail in Tables I and II.

[4]We also note that some of the intermediate symmetry breaking chains involving $SO(10)$ GUTs may give rise to cosmic strings which give rise to GW spectrum and the signals from induced GW spectrum presented in this paper and those may add up to give a combined signal while some breaking chains will not have generation of cosmic strings. All these depend upon the specific chain and the scale of symmetry breaking. Such a study is beyond the scope of present study. For details see [103,104].

observables are given in Tables I and II. However detailed analysis of such studies involving other gauge groups is beyond the scope of the present manuscript and we leave it for future publication. It is worth mentioning that magnetic monopoles that are produced due to $SU(5)$ symmetry breaking are inflated away in our scenario, since the gauge symmetry is broken during inflation via the inflaton coupling to the adjoint Higgs.

IV. INFLATIONARY PERTURBATIONS AND CMB

In this section, we study the inflationary perturbations and their cosmological consequences. In particular, we aim to investigate the generation of sufficiently large scalar fluctuations that may lead to PBH production within the realm of our inflationary scenario. In this case, inflation proceeds in two or more phases of slow roll (SR) which should be separated in between by a brief exit from the SR phase and a transient USR phase. In this scenario, scalar modes that exit the horizon are enhanced [105,106]. The latter enhancement controls the position and height of the generated peak in the scalar power spectrum, and in turn may form PBHs with varying mass scales and scalar induced GWs at different frequencies.

A. Curvature perturbations

We start by giving the form of perturbed metric as follows:

$$ds^2 = a(\tau)^2\left[-(1+2\Phi)d\tau^2 + \left((1-2\Psi)\delta_{ij} + \frac{1}{2}h_{ij}\right)dx^i dx^j\right], \tag{25}$$

where h_{ij} are the tensor perturbations, while Φ and Ψ are called the Bardeen potentials, which are equal in the conformal Newtonian gauge.

Now we study the evolution of the scalar curvature perturbation $\mathcal{R}_c$ by defining the Mukhanov field $v \equiv z\mathcal{R}_c$, with $z \equiv a\dot{\phi}/H$, and a is the scale factor [55].

In this respect, the evolution of Fourier modes of v is given by the Mukhanov-Sasaki (MS) equations [107–109],

$$v_k'' + \left(k^2 - \frac{z''}{z}\right)v_k = 0, \tag{26}$$

where the prime in the last equation means differentiation with respect to conformal time that is defined by, $d\tau \equiv dt/a$.[5] The factor $(k^2 - \frac{z''}{z})$ is considered to be an effective frequency $\omega_k^2(\tau)$. It is convenient to express the factor $\frac{z''}{z}$ that is important to study the evolution of the modes, in terms of the SR parameters as follows:

$$\frac{z''}{z} = \mathcal{H}^2[2 - (3-\epsilon_H)\eta_V + \epsilon_H(5 + 2\epsilon_H - 4\eta_H)], \tag{27}$$

where $\mathcal{H} \equiv a'/a = aH$. It is worth mentioning that this expression is exact to all orders in the SR parameters. Also, we note that during the SR phase, the SR parameters are very small, and therefore $z''/z \approx 2\mathcal{H}^2$.

We recognize two phases for the evolution of the modes; the subhorizon evolution phase where $k^2 \gg z''/z$, and the superhorizon evolution phase $k^2 \ll z''/z$. In the subhorizon limit, the mode v_k behaves as a free field in flat spacetime. Therefore, in the Bunch-Davies vacuum, the normalized solution is

$$v_k = \frac{1}{\sqrt{2k}}e^{-ik\tau}. \tag{28}$$

We use this free solution as the initial condition when solving the MS equation. On the other hand, in the superhorizon limit, the general solution can be written as a linear combination [110]

$$v_k = A_{1,k}v_0^{(1)} + A_{2,k}v_0^{(2)}, \tag{29}$$

where the mode $v_0^{(1)}$ grows during SR, while the mode $v_0^{(2)}$ decays during SR. They are expressed as [110]

$$v_0^{(1)} \propto z, \qquad v_0^{(2)} \propto z\int_\tau^0 \frac{d\tau'}{z(\tau')^2}. \tag{30}$$

Therefore, $v_0^{(1)}$ will finally dominate and hence, the amplitude of the curvature perturbations is frozen [110]

$$|\mathcal{R}_{ck}| = |v_k/z| = \text{const.} \tag{31}$$

Now let us discuss what happens when SR is momentarily violated. In that case, the growing and decreasing v_k modes can mix if z decreases as advocated in [110]. Accordingly, the second mode may come to dominate momentarily, which may lead to a superhorizon evolution of $\mathcal{R}_c$. At the end of this temporary phase, z starts to grow, and again, $\mathcal{R}_c$ will be frozen. In this case, we can link the observable perturbations at horizon reentry to the perturbations produced during inflation.

The primordial power spectrum is computed after the time of horizon crossing as studied in details in Refs. [55,110], and is given by

$$\mathcal{P}_\xi = \frac{k^3}{2\pi^2}\frac{|v_k|^2}{z^2}\bigg|_{\mathcal{H}\gg k} \overset{\text{SR}}{\approx} \frac{H^2}{8\pi^2 M_{\text{P}}^2\epsilon_H}\bigg|_{k=\mathcal{H}}. \tag{32}$$

Now, we can replace the Hubble SR parameters ϵ_H and η_H, by the potential SR parameters ϵ_V and η_V. Therefore, the scalar spectral index n_s and the tensor-to-scalar ratio r are given at the leading order in SR by

[5]This should not be confused with the prime in V', which corresponds to a derivative with respect to the scalar field.

$$n_s \approx 1 + 2\eta_V - 6\epsilon_V, \qquad r \approx 16\epsilon_V. \tag{33}$$

The recent CMB observational constraints on inflationary observables are given at the pivot scale $k_{\rm pivot} = 0.05\ {\rm Mpc}^{-1}$ [111,112], as follows:

$$A_s = (2.10 \pm 0.03) \times 10^{-9}, \qquad n_s = 0.9649 \pm 0.0042, \qquad r < 0.036. \tag{34}$$

As a matter of fact, the curvature power spectrum is constrained at scales relevant for the CMB. Therefore, we define

$$A_s \equiv \mathcal{P}_\xi(k_{\rm pivot}) = 2.1 \times 10^{-9}. \tag{35}$$

B. Inflationary background dynamics and spectrum of curvature perturbations

Here, we discuss the solution of the MS equation in order to calculate the primordial power spectrum. We first solve the background equation of motion of the canonical inflaton field σ together with Friedmann equations,

$$\ddot{\sigma} + 3H\dot{\sigma} + \frac{dV}{d\sigma} = 0, \qquad 3H^2 = \frac{1}{M_{\rm Pl}^2}\left[\frac{1}{2}\dot{\sigma}^2 + V(\sigma)\right], \tag{36}$$

where dot denotes the derivative with respect to the cosmic time. We define the number of e-folds N as $dN = Hdt$ and rewrite Eq. (36) to be merged into one equation as follows:

$$\frac{d^2\sigma}{dN^2} + 3\frac{d\sigma}{dN} - \left[3 - \frac{1}{2}\left(\frac{d\sigma}{dN}\right)^2\right]\frac{V'(\sigma)}{V(\sigma)} = 0, \tag{37}$$

where we set $M_{\rm Pl}^2 = 1$. The Hubble SR parameters can be given in terms of N as well, by

$$\epsilon_H \equiv \frac{1}{2}\frac{\dot{\sigma}^2}{H^2} = \frac{1}{2}\left(\frac{d\sigma}{dN}\right)^2, \tag{38}$$

$$\eta_H \equiv -\frac{\ddot{\sigma}}{H\dot{\sigma}} = \epsilon_H - \frac{1}{2\epsilon_H}\frac{d\epsilon_H}{dN}. \tag{39}$$

The scalar spectral index and the tensor to scalar ratio are then given respectively by

$$n_s \approx 1 - 4\epsilon_H + 2\eta_H, \qquad r \approx 16\epsilon_H. \tag{40}$$

In our numerical treatment, we rewrite the background equation of motion in terms of x as follows[6]:

$$v\left[\frac{d\sigma}{d\phi}\frac{d^2x}{dN^2} + v\frac{d^2\sigma}{d\phi^2}\left(\frac{dx}{dN}\right)^2\right] + v\frac{d\sigma}{d\phi}\frac{dx}{dN}\left[3 - \frac{1}{2}v^2\left(\frac{d\sigma}{d\phi}\right)^2\left(\frac{dx}{dN}\right)^2\right] + \frac{1}{v}\frac{d\phi}{d\sigma}\left[3 - \frac{1}{2}v^2\left(\frac{d\sigma}{d\phi}\right)^2\left(\frac{dx}{dN}\right)^2\right]\frac{V'(x)}{V(x)} = 0. \tag{41}$$

Moreover, we study the evolution of the curvature perturbations by numerically solving the MS equation that is rewritten in terms of N as [66]

$$\frac{d^2v_k}{dN^2} + (1-\epsilon_H)\frac{dv_k}{dN} + \left[\frac{k^2}{e^{2N}H^2} + (1+\epsilon_H-\eta_H)(\eta_H-2) - \frac{d(\epsilon_H-\eta_H)}{dN}\right]v_k = 0. \tag{42}$$

We can then compute the power spectrum at the end of inflation as

$$\mathcal{P}_\zeta(k) = \frac{k^3}{2\pi^2}\left|\frac{v_k}{z}\right|^2_{N=N_{\rm end}}. \tag{43}$$

As we advocated above, we choose suitable initial conditions by assuming the Bunch-Davies vacuum at very early times [55,113],

$$\lim_{\tau\to-\infty} v_k = \frac{e^{-ik\tau}}{\sqrt{2k}}. \tag{44}$$

Therefore, we have

$${\rm Re}(v_k)|_{N=N_i} = \frac{1}{\sqrt{2k}}; \qquad {\rm Im}(v_k)|_{N=N_i} = 0, \tag{45}$$

$${\rm Re}\left(\frac{dv_k}{dN}\right)\Big|_{N=N_i} = 0, \quad {\rm Im}\left(\frac{dv_k}{dN}\right)\Big|_{N=N_i} = -\frac{\sqrt{k}}{\sqrt{2}a(N_i)H(N_i)}, \tag{46}$$

where N_i is the initial value of N where we start the numerical integration of the MS equation.

C. Numerical results

We are ready to present our numerical results for the primordial perturbations and the power spectrum. We choose three benchmark points with a nonzero values of the inflaton VEV, as shown in Table I.[7] We have chosen

[6]This equation is similar to Eq. (37) in [55].

[7]Such choice of values may incur some fine-tuning.

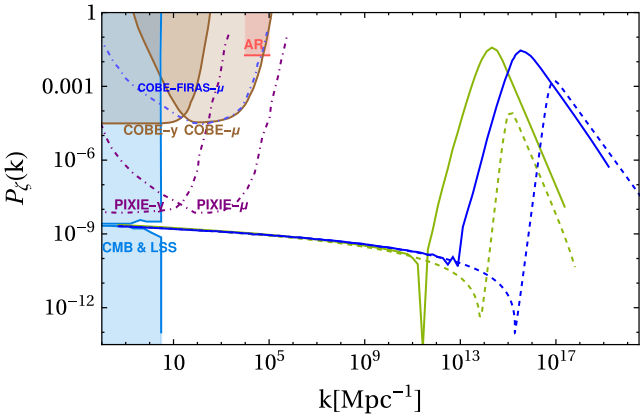

FIG. 4. The power spectrum calculated using the benchmark points in Table I, solid green for $v = 0.1M_{Pl}$, and solid blue for $v = 0.8M_{Pl}$, by solving the exact equations for perturbations (Mukhanov-Sasaki equations). The dashed curves represent the corresponding power spectra calculated in the slow-roll approximation. The shaded regions represent the constraints from current observations, while the dot-dashed curves represent future constraints [114–118].

consistent inflaton VEV values that generates a reasonable peak in the power spectrum and induces GUT symmetry breaking at the scale $M_{GUT} \geq 5 \times 10^{15}$. We have calculated the CMB observables at the pivot scale $k_* = 0.05$ Mpc^{-1} as presented in Table II. We solve the background equations numerically with inflation ending at $\epsilon_H = 1$. For the initial velocity, we set $x'(0) = 0$, and we chose the initial field value $x(0)$ such that the peak in the power spectrum occurs at $k \sim 10^{14}$ Mpc^{-1}, such that the PBH mass is larger than 10^{16} g. This fixes the inflation observable values shown in Table II. In Fig. 4, we display the power spectrum P_ζ versus the scale k. As indicated in the figure, the curvature power spectrum is constrained at scales 10^{-4} Mpc$^{-1} \lesssim k \lesssim 1$ Mpc^{-1}, due to CMB observations. We use two values of the inflaton VEV, $v = 0.1M_{Pl}$ and $0.8M_{Pl}$, as well as the model parameters in Table I. The solid curves are generated by numerically solving the MS equation (42), and the dashed curves are due to SR considerations.

V. SCALAR-INDUCED GRAVITATIONAL WAVES AND PRIMORDIAL BLACK HOLES

In this section, we study the scalar-induced gravitational waves (GWs) due to the enhancement in the primordial power spectrum. Indeed, second-order tensor perturbations are sourced from enhanced scalar perturbations. The height of the power spectrum peaks as well as their position at scale, k_{peak}, are dictated by the scalar-potential parameters, including the inflaton VEV v, which in turn is intimately related to the gauge symmetry-breaking scale M_{SB}, including the GUT scale. Therefore, these symmetry breaking scales can be probed via scalar-induced gravitational waves. Here, we assume that the gravitational waves were formed during the radiation-dominated epoch.[8]

We follow [91,93,119–121] in our numerical calculations of the spectrum of the scalar induced GWs. Using the primordial power spectrum $\mathcal{P}_\zeta$, the scalar induced GWs spectrum is given by [120]

$$\Omega_{GW}^{si}h^2 \approx 4.6 \times 10^{-4}\left(\frac{g_{*,s}^4 g_*^{-3}}{100}\right)^{-\frac{1}{3}} \int_{-1}^{1} dx \int_{1}^{\infty} dy \mathcal{P}_\zeta\left(\frac{y-x}{2}k\right)\mathcal{P}_\zeta\left(\frac{x+y}{2}k\right)F(x,y)\Big|_{k=2\pi f}, \tag{47}$$

where $g_{*,s}$ and g_* are the effective numbers of relativistic energy and entropy degrees of freedom and we will take $g_{*,s} \approx g_*$. The function F is defined by

$$F(x,y) = \frac{(x^2+y^2-6)^2(x^2-1)^2(y^2-1)^2}{(x-y)^8(x+y)^8} \times \left\{\left[x^2-y^2+\frac{x^2+y^2-6}{2}\ln\left|\frac{y^2-3}{x^2-3}\right|\right]^2 + \frac{\pi^2(x^2+y^2-6)^2}{4}\theta(y-\sqrt{3})\right\}. \tag{48}$$

After calculating the power spectrum as explained in the previous section, we feed it into Eq. (47) in order to calculate the GWs energy density. In Fig. 5 we plot the energy density of GWs, using Eq. (47), versus the frequency. The figure shows that the predicted GW spectra for the parameter choices in Table I, lie well within the detection range of future GW experiments like LISA, DECIGO, BBO, SKA, and ET [122–126].

Beside probing the GUT scale or other gauge symmetry breaking scales via the observable energy density of GWs,

[8]Gravitational waves can arise also from $SU(5)$ GUT phase transition, if they are at all of strong first order. However, the produced gravitational waves are at very high frequency and hence not detectable in the currently proposed GW detectors and also do not affect the GW spectrum presented in Fig. 5.

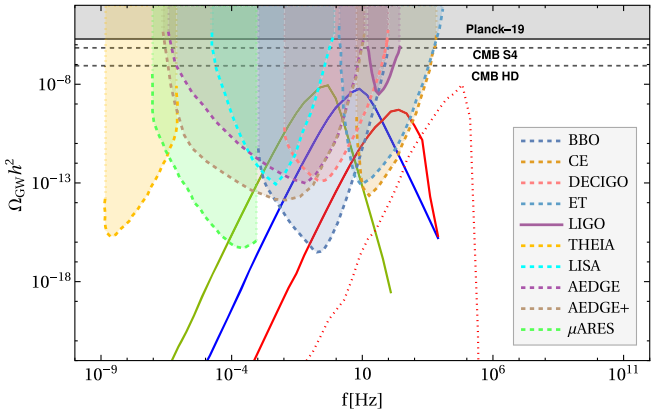

FIG. 5. The spectrum of scalar-induced gravitational waves (solid red, blue, and green curves for $v = 0.1M_{Pl}, 0.8M_{Pl}, 10M_{Pl}$) versus current and future GW detectors constraints. We have used the parameter values in Table I. The red dotted curve corresponds to $v = 10M_{Pl}$, but with a modified value of the tensor to scalar ratio, $r \sim 0.064$.

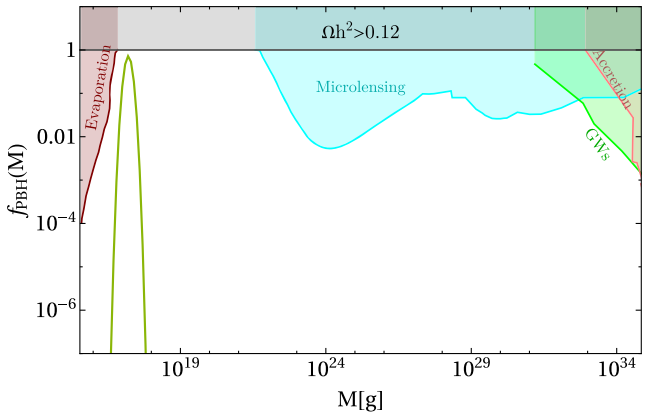

FIG. 6. The fractional abundance of PBHs as a function of their mass corresponding to the parameter values in Table I, with the inflaton VEV, $v = 0.1M_{Pl}$. The shaded regions correspond to the observational constraints [79,148,149]. PBHs generated by other benchmark points with larger VEV values, such as $v = 0.8M_{Pl}$ and $v = 10M_{Pl}$, are expected to evaporate before BBN.

as described above, the significant enhancement of the scalar power spectrum can lead to copious production of PBHs. As shown in Ref. [127], the GWs spectrum can be related to a prediction for the PBH abundance as DM. Therefore, we calculate the mass of PBHs and their fractional energy density abundances. We will assume that the PBHs were formed during the radiation-dominated epoch, just like the gravitational waves.

Following Ref. [128], the fractional abundance of PBHs, Ω_{PBH}/Ω_{DM}, is defined to be

$$\frac{\Omega_{PBH}}{\Omega_{DM}}(M_{PBH}) = \frac{\beta(M_{PBH})}{8\times10^{-16}}\left(\frac{\gamma}{0.2}\right)^{3/2}\left(\frac{g_*(T_f)}{106.75}\right)^{-1/4} \times\left(\frac{M_{PBH}}{10^{-18}\ \text{grams}}\right)^{-1/2}, \tag{49}$$

where M_{PBH} denotes the PBH mass, $\Omega_{DM} \simeq 0.26$ is the DM abundance, and the factor γ represents the dependence on the gravitation collapse and is set to be equal to 0.2 [58]. The function $\beta(M_{PBH})$ shows the mass fraction of Universe collapsing into PBH. T_f represents the temperature at which PBHs are formed, and $g_*(T_f)$ denotes the effective degrees of freedom during the formation of PBHs. The fractional abundance of PBHs f_{PBH} is then given by [128]

$$f_{PBH} = \int \frac{dM_{PBH}}{M_{PBH}}\frac{\Omega_{PBH}}{\Omega_{DM}}. \tag{50}$$

After inflation ends, the modes re-enter the Hubble horizon H^{-1} and PBHs are formed. With the assumption of spherical collapse of perturbations, we have [66]

$$M_{PBH} = \gamma\frac{4\pi\rho}{3}H^{-3}. \tag{51}$$

Here ρ is the energy density of Universe during collapse to form PBHs. For PBHs created during the radiation epoch, the PBHs mass is given (in grams) as a function of the comoving wave number k [66,128], as follows:

$$M_{PBH}(k) = 10^{18}\left(\frac{\gamma}{0.2}\right)\left(\frac{g_*(T_f)}{106.75}\right)^{-1/6}\left(\frac{k}{7\times10^{13}\,\text{Mpc}^{-1}}\right)^{-2}. \tag{52}$$

The factor $g_*(T) = 106.75$ in case we assume the SM spectrum. However, with a spectrum of $SU(5)$ GUT as we have in our scenario, we set $g_*(T) = 228.75$. Thus the PBH fractional abundance in the SM is 1.13 times larger than in the $SU(5)$. This relative factor, to a good approximation, can be safely ignored.

We follow the Press-Schechter approach in order to evaluate the mass fraction β. Assuming that, the over-density δ follows a Gaussian probability distribution function, β can be calculated from the following integral

$$\beta(M_{PBH}) = \frac{1}{\sqrt{2\pi\sigma^2(M_{PBH})}}\int_{\delta_c}^{\infty} d\delta \exp\left(-\frac{\delta^2}{2\sigma^2(M_{PBH})}\right), \tag{53}$$

with δ_c being a threshold for the PBH collapse, and σ is the variance of the curvature perturbation, which can be written in terms of the comoving wave number as follows:

$$\sigma^2(M_{PBH}(k)) = \frac{16}{81}\int\frac{dk'}{k'}\left(\frac{k'}{k}\right)^4 P_R(k')\tilde{W}\left(\frac{k'}{k}\right), \tag{54}$$

where the window function $\tilde{W}(x)$ can be approximated with a Gaussian distribution function to be: $\tilde{W}(x) = e^{-x^2/2}$.

For δ_c, following Refs. [129–136], we have taken its values in the range between 0.4 and 0.6.

Figure 6 depicts the fractional abundance of the primordial black holes as a function of their mass. We have used only one benchmark point (BP) for the parameters of Table I, corresponding to $v = 0.1\mathrm{M_{Pl}}$. The PBHs generated by other benchmark points with larger VEV values, such as $v = 0.8M_{\mathrm{Pl}}$ and $v = 10M_{\mathrm{Pl}}$, are expected to evaporate before BBN, and may not serve as the DM candidate (whole or partially). The figure shows that PBH abundance can account for the observed DM relic density for PBH mass scale $\sim 10^{17}$ g $\simeq 5 \times 10^{-17} M_\odot$, where $M_\odot$ is the solar mass. The shaded regions are disallowed by observations from Planck, acccretion disk, microlensing, gravitational waves, and black hole evaporation and several other constraints [79,137–149].

VI. DISCUSSION AND CONCLUSIONS

In this paper we present a single-field inflection-point model of $SU(5)$ inflation. The inflaton is a $SU(5)$ gauge-singlet which couples to the $SU(5)$ Higgs responsible for $SU(5)$-symmetry breaking induced via the Higgs-portal mixed quartic coupling. As the inflaton rolls down to its potential minimum, the $SU(5)$ symmetry is also broken leading to a one-to-one correspondence between the GUT scale and the scale of inflection point via the inflaton VEV. We show that such an inflationary scenario may lead to the generation of both detectable GWs and sufficient PBHs as the sole DM candidate of the Universe. We summarize our main findings below:

(i) The scale of grand unification which is otherwise very challenging to probe in laboratory experiments is highly constrained. We investigated a cosmological scenario in $SU(5)$ which provides a pathway to probe the $SU(5)$ gauge symmetry breaking scale via inflationary observables. We show this for a model involving inflection-point inflation employing an $SU(5)$ singlet Higgs nonminimally coupled to the Ricci scalar. We predict the CMB observables with respect to the choice of GUT scale M_{GUT} (see Table II). The prediction r $\approx$0.026 for tensor-to-scalar ratio, will be within reach of the next generation CMB experiments for our choice of the benchmark point.

(ii) Since the $SU(5)$ scalar singlet acquires a VEV and mixes with the $SU(5)$ adjoint higgs which breaks symmetry to the SM, we expect quantum corrections to the self-quartic couplings from gauge interactions. Constraints on such couplings from quantum corrections in this scenario have been estimated (see Sec. III). We also discuss implications for models based on gauge groups such as $SU(4)_C \times SU(2)_L \times SU(2)_R$ and $SU(3)_C \times SU(3)_L \times SU(3)_R$, which can accommodate symmetry-breaking scales lower than M_{GUT}.

(iii) We estimate the power spectrum across all k-values which provides constraints on the $SU(5)$ model from the measurements of CMB spectral distortions (see Fig. 4). The power spectrum shows a spike in the amplitude which corresponds to the $SU(5)$ symmetry breaking scale via its relation with the inflection-point and the inflaton rolling to its minima and completing the $SU(5)$ symmetry breaking.

(iv) Second-order tensor perturbations propagate as GW that are detectable with $\Omega_{\mathrm{GW}}h^2 \sim 10^{-9}$ and peak frequency $f \sim 0.1$ Hz by LISA and $\Omega_{\mathrm{GW}}h^2 \sim 10^{-10}$ and peak frequency of $\sim$10 Hz in ET. Furthermore, in other next generation GW observatories such as AEDGE, BBO, DECIGO, one may be able to detect this signal, and this will act as a novel probe of GUT scale physics (see Fig. 5).

(v) Production of PBH of masses 10^{17}–10^{18} g $(10 - 100M_\odot)$ as the sole DM candidate in the Universe is proposed. This novel DM candidate is also a signature of scale of grand unification involving inflationary cosmology (see Fig. 6).

We believe that the precision that GW astronomy aspires from the planned worldwide network of GW detectors can make the dream of testing high-scale and fundamental BSM scenarios of UV completion like grand unification a reality which complement the laboratory searches in near future.

ACKNOWLEDGMENTS

The work of A. M. is supported in part by the Science, Technology and Innovation Funding Authority (STDF) under Grant No. 33495. The authors thank Amit Tiwari and Shiladitya Porey for carefully reading the manuscript.

[1] S. Weinberg, Phys. Rev. Lett. **43**, 1566 (1979).
[2] F. Wilczek and A. Zee, Phys. Rev. Lett. **43**, 1571 (1979).
[3] S. Weinberg, Phys. Rev. D **22**, 1694 (1980).
[4] S. Weinberg, Phys. Rev. D **26**, 287 (1982).
[5] N. Sakai and T. Yanagida, Nucl. Phys. **B197**, 533 (1982).
[6] S. Dimopoulos, S. Raby, and F. Wilczek, Phys. Lett. **112B**, 133 (1982).
[7] J. R. Ellis, D. V. Nanopoulos, and S. Rudaz, Nucl. Phys. **B202**, 43 (1982).

[8] K. Abe *et al.* (Super-Kamiokande Collaboration), Phys. Rev. D **90**, 072005 (2014).
[9] K. Abe *et al.* (Super-Kamiokande Collaboration), Phys. Rev. D **95**, 012004 (2017).
[10] R. Acciarri *et al.* (DUNE Collaboration), arXiv:1512.06148.
[11] K. Abe *et al.* (Hyper-Kamiokande Collaboration), arXiv:1805.04163.
[12] F. An *et al.* (JUNO Collaboration), J. Phys. G **43**, 030401 (2016).
[13] K. Sato, Mon. Not. R. Astron. Soc. **195**, 467 (1981).
[14] V. Petrosian, Report No. PRINT-82-0526 (Stanford).
[15] A. H. Guth, Phys. Rev. D **23**, 347 (1981).
[16] A. D. Linde, Phys. Lett. **108B**, 389 (1982).
[17] H. Nariai, Report No. RRK-72-6.
[18] A. A. Starobinsky, Phys. Lett. **91B**, 99 (1980).
[19] Q. Shafi and A. Vilenkin, Phys. Rev. Lett. **52**, 691 (1984).
[20] G. Lazarides and Q. Shafi, Phys. Lett. **148B**, 35 (1984).
[21] T. W. B. Kibble, G. Lazarides, and Q. Shafi, Phys. Lett. **113B**, 237 (1982).
[22] Q. Shafi and A. Vilenkin, Phys. Rev. D **29**, 1870 (1984).
[23] G. Lazarides, M. Magg, and Q. Shafi, Phys. Lett. **97B**, 87 (1980).
[24] R. Maji and Q. Shafi, J. Cosmol. Astropart. Phys. 03 (2023) 007.
[25] G. Lazarides, R. Maji, R. Roshan, and Q. Shafi, J. Cosmol. Astropart. Phys. 12 (2022) 009.
[26] V. N. Şenoğuz and Q. Shafi, Phys. Lett. B **752**, 169 (2016).
[27] G. Lazarides and Q. Shafi, J. High Energy Phys. 10 (2019) 193.
[28] K. Sravan Kumar and P. Vargas Moniz, Eur. Phys. J. C **79**, 945 (2019).
[29] S. Biondini and K. Sravan Kumar, J. High Energy Phys. 07 (2020) 039.
[30] S. Kawai and J. Kim, Phys. Rev. D **93**, 065023 (2016).
[31] F. L. Bezrukov and M. Shaposhnikov, Phys. Lett. B **659**, 703 (2008).
[32] V. V. Khoze, J. High Energy Phys. 11 (2013) 215.
[33] K. Kannike, A. Racioppi, and M. Raidal, J. High Energy Phys. 06 (2014) 154.
[34] M. Rinaldi, G. Cognola, L. Vanzo, and S. Zerbini, Phys. Rev. D **91**, 123527 (2015).
[35] A. Salvio and A. Strumia, J. High Energy Phys. 06 (2014) 080.
[36] K. Kannike, G. Hütsi, L. Pizza, A. Racioppi, M. Raidal, A. Salvio, and A. Strumia, J. High Energy Phys. 05 (2015) 065.
[37] K. Kannike, G. Hütsi, L. Pizza, A. Racioppi, M. Raidal, A. Salvio, and A. Strumia, Proc. Sci. EPS-HEP2015 (**2015**) 379.
[38] N. D. Barrie, A. Kobakhidze, and S. Liang, Phys. Lett. B **756**, 390 (2016).
[39] G. Tambalo and M. Rinaldi, Gen. Relativ. Gravit. **49**, 52 (2017).
[40] I. D. Novikov, A. G. Polnarev, A. A. Starobinskii, and I. B. Zeldovich, Astron. Astrophys. **80**, 104 (1979).
[41] G. F. Chapline, Nature (London) **253**, 251 (1975).
[42] A. Dolgov and J. Silk, Phys. Rev. D **47**, 4244 (1993).
[43] K. Jedamzik, Phys. Rev. D **55**, R5871 (1997).
[44] P. Ivanov, P. Naselsky, and I. Novikov, Phys. Rev. D **50**, 7173 (1994).
[45] J. Garcia-Bellido, A. D. Linde, and D. Wands, Phys. Rev. D **54**, 6040 (1996).
[46] J. Yokoyama, Astron. Astrophys. **318**, 673 (1997).
[47] P. Ivanov, Phys. Rev. D **57**, 7145 (1998).
[48] D. Blais, C. Kiefer, and D. Polarski, Phys. Lett. B **535**, 11 (2002).
[49] L. Heurtier, A. Moursy, and L. Wacquez, J. Cosmol. Astropart. Phys. 03 (2023) 020.
[50] J. W. Chen, M. Zhu, S. F. Yan, Q. Q. Wang, and Y. F. Cai, J. Cosmol. Astropart. Phys. 01 (2023) 015.
[51] S. Choudhury and A. Mazumdar, Phys. Lett. B **733**, 270 (2014).
[52] W. Ahmed, M. Junaid, and U. Zubair, Nucl. Phys. **B984**, 115968 (2022).
[53] S. Kawai and J. Kim, Phys. Rev. D **104**, 083545 (2021).
[54] S. Kawai and J. Kim, Phys. Rev. D **104**, 043525 (2021).
[55] M. Drees and Y. Xu, Eur. Phys. J. C **81**, 182 (2021).
[56] B. P. Abbott *et al.* (LIGO Scientific and Virgo Collaborations), Phys. Rev. X **6**, 041015 (2016); **8**, 039903(E) (2018).
[57] B. J. Carr and S. W. Hawking, Mon. Not. R. Astron. Soc. **168**, 399 (1974).
[58] B. J. Carr, Astrophys. J. **201**, 1 (1975).
[59] J. Garcia-Bellido and E. Ruiz Morales, Phys. Dark Universe **18**, 47 (2017).
[60] J. M. Ezquiaga, J. Garcia-Bellido, and E. Ruiz Morales, Phys. Lett. B **776**, 345 (2018).
[61] K. Kannike, L. Marzola, M. Raidal, and H. Veermäe, J. Cosmol. Astropart. Phys. 09 (2017) 020.
[62] C. Germani and T. Prokopec, Phys. Dark Universe **18**, 6 (2017).
[63] H. Motohashi and W. Hu, Phys. Rev. D **96**, 063503 (2017).
[64] H. Di and Y. Gong, J. Cosmol. Astropart. Phys. 07 (2018) 007.
[65] S. Rasanen and E. Tomberg, J. Cosmol. Astropart. Phys. 01 (2019) 038.
[66] G. Ballesteros and M. Taoso, Phys. Rev. D **97**, 023501 (2018).
[67] J. Kristiano and J. Yokoyama, arXiv:2211.03395.
[68] A. Riotto, arXiv:2301.00599.
[69] J. Kristiano and J. Yokoyama, arXiv:2303.00341.
[70] A. Riotto, arXiv:2303.01727.
[71] S. Choudhury, S. Panda, and M. Sami, J. Cosmol. Astropart. Phys. 08 (2023) 078.
[72] S. Choudhury, S. Panda, and M. Sami, arXiv:2303.06066.
[73] S. Choudhury, S. Panda, and M. Sami, Phys. Lett. B **845**, 138123 (2023).
[74] S. Choudhury, M. R. Gangopadhyay, and M. Sami, arXiv:2301.10000.
[75] G. Franciolini, A. Iovino, Jr., M. Taoso, and A. Urbano, arXiv:2305.03491.
[76] J. Fumagalli, arXiv:2305.19263.
[77] B. Carr, M. Raidal, T. Tenkanen, V. Vaskonen, and H. Veermäe, Phys. Rev. D **96**, 023514 (2017).
[78] B. Carr, F. Kuhnel, and M. Sandstad, Phys. Rev. D **94**, 083504 (2016).
[79] B. J. Carr, K. Kohri, Y. Sendouda, and J. Yokoyama, Phys. Rev. D **81**, 104019 (2010).
[80] N. Bartolo, V. De Luca, G. Franciolini, A. Lewis, M. Peloso, and A. Riotto, Phys. Rev. Lett. **122**, 211301 (2019).

[81] F. Hajkarim and J. Schaffner-Bielich, Phys. Rev. D **101**, 043522 (2020).
[82] J. Liu, Z. K. Guo, and R. G. Cai, Phys. Rev. D **101**, 083535 (2020).
[83] W. T. Xu, J. Liu, T. J. Gao, and Z. K. Guo, Phys. Rev. D **101**, 023505 (2020).
[84] C. Fu, P. Wu, and H. Yu, Phys. Rev. D **101**, 023529 (2020).
[85] N. Bartolo, V. De Luca, G. Franciolini, M. Peloso, D. Racco, and A. Riotto, Phys. Rev. D **99**, 103521 (2019).
[86] S. Clesse, J. García-Bellido, and S. Orani, arXiv: 1812.11011.
[87] M. Braglia, D. K. Hazra, F. Finelli, G. F. Smoot, L. Sriramkumar, and A. A. Starobinsky, J. Cosmol. Astropart. Phys. 08 (2020) 001.
[88] N. Bhaumik, A. Ghoshal, and M. Lewicki, J. High Energy Phys. 07 (2022) 130.
[89] N. Bhaumik, A. Ghoshal, R. K. Jain, and M. Lewicki, J. High Energy Phys. 05 (2023) 169.
[90] C. Chen, A. Ghoshal, Z. Lalak, Y. Luo, and A. Naskar, J. Cosmol. Astropart. Phys. 08 (2023) 041.
[91] K. Kohri and T. Terada, Phys. Rev. D **97**, 123532 (2018).
[92] G. Ferrante, G. Franciolini, A. Iovino, Jr., and A. Urbano, J. Cosmol. Astropart. Phys. 06 (2023) 057.
[93] A. Chatterjee and A. Mazumdar, Phys. Rev. D **97**, 063517 (2018).
[94] R. g. Cai, S. Pi, and M. Sasaki, Phys. Rev. Lett. **122**, 201101 (2019).
[95] J. C. Pati and A. Salam, Phys. Rev. D **8**, 1240 (1973).
[96] S. L. Glashow, Trinification of all elementary particle forces, Report No. Print-84-0577 (Boston).
[97] K. S. Babu, X. G. He, and S. Pakvasa, Phys. Rev. D **33**, 763 (1986).
[98] G. R. Dvali and Q. Shafi, Supersymmetric trinification and low energy consequences.
[99] J. J. Blanco-Pillado, K. D. Olum, and B. Shlaer, Phys. Rev. D **89**, 023512 (2014).
[100] N. Aghanim *et al.* (Planck Collaboration), Astron. Astrophys. **641**, A6 (2020); **652**, C4(E) (2021).
[101] P. A. R. Ade *et al.* (BICEP/Keck Collaboration), arXiv: 2203.16556.
[102] B. Bhattacherjee, P. Byakti, A. Kushwaha, and S. K. Vempati, J. High Energy Phys. 05 (2018) 090.
[103] S. F. King, S. Pascoli, J. Turner, and Y. L. Zhou, Phys. Rev. Lett. **126**, 021802 (2021).
[104] S. F. King, S. Pascoli, J. Turner, and Y. L. Zhou, J. High Energy Phys. 10 (2021) 225.
[105] S. M. Leach and A. R. Liddle, Phys. Rev. D **63**, 043508 (2001).
[106] S. M. Leach, M. Sasaki, D. Wands, and A. R. Liddle, Phys. Rev. D **64**, 023512 (2001).
[107] V. F. Mukhanov, JETP Lett. **41**, 493 (1985).
[108] M. Sasaki, Prog. Theor. Phys. **76**, 1036 (1986).
[109] V. F. Mukhanov, H. A. Feldman, and R. H. Brandenberger, Phys. Rep. **215**, 203 (1992).
[110] A. Karam, N. Koivunen, E. Tomberg, V. Vaskonen, and H. Veermäe, J. Cosmol. Astropart. Phys. 03 (2023) 013.
[111] Y. Akrami *et al.* (Planck Collaboration), Astron. Astrophys. **641**, A10 (2020).
[112] P. A. R. Ade *et al.* (BICEP/Keck Collaboration), Phys. Rev. Lett. **127**, 151301 (2021).
[113] T. S. Bunch and P. C. W. Davies, Proc. R. Soc. A **360**, 117 (1978).
[114] J. Chluba, A. L. Erickcek, and I. Ben-Dayan, Astrophys. J. **758**, 76 (2012).
[115] J. Chluba and D. Grin, Mon. Not. R. Astron. Soc. **434**, 1619 (2013).
[116] D. J. Fixsen, E. S. Cheng, J. M. Gales, J. C. Mather, R. A. Shafer, and E. L. Wright, Astrophys. J. **473**, 576 (1996).
[117] A. Kogut, D. J. Fixsen, D. T. Chuss, J. Dotson, E. Dwek, M. Halpern, G. F. Hinshaw, S. M. Meyer, S. H. Moseley, M. D. Seiffert *et al.*, J. Cosmol. Astropart. Phys. 07 (2011) 025.
[118] F. Bianchini and G. Fabbian, Phys. Rev. D **106**, 063527 (2022).
[119] J. R. Espinosa, D. Racco, and A. Riotto, J. Cosmol. Astropart. Phys. 09 (2018) 012.
[120] M. Lewicki, O. Pujolàs, and V. Vaskonen, Eur. Phys. J. C **81**, 857 (2021).
[121] K. Inomata and T. Terada, Phys. Rev. D **101**, 023523 (2020).
[122] P. Amaro-Seoane *et al.* (LISA Collaboration), arXiv: 1702.00786.
[123] K. Yagi and N. Seto, Phys. Rev. D **83**, 044011 (2011); **95**, 109901(E) (2017).
[124] S. Sato, S. Kawamura, M. Ando, T. Nakamura, K. Tsubono, A. Araya, I. Funaki, K. Ioka, N. Kanda, S. Moriwaki *et al.*, J. Phys. Conf. Ser. **840**, 012010 (2017).
[125] B. S. Sathyaprakash and B. F. Schutz, Living Rev. Relativity **12**, 2 (2009).
[126] W. Zhao, Y. Zhang, X. P. You, and Z. H. Zhu, Phys. Rev. D **87**, 124012 (2013).
[127] V. De Luca, G. Franciolini, and A. Riotto, Phys. Rev. Lett. **126**, 041303 (2021).
[128] V. C. Spanos and I. D. Stamou, Phys. Rev. D **104**, 123537 (2021).
[129] T. Harada, C. M. Yoo, and K. Kohri, Phys. Rev. D **88**, 084051 (2013); **89**, 029903(E) (2014).
[130] I. Musco, J. C. Miller, and A. G. Polnarev, Classical Quantum Gravity **26**, 235001 (2009).
[131] I. Musco, J. C. Miller, and L. Rezzolla, Classical Quantum Gravity **22**, 1405 (2005).
[132] I. Musco and J. C. Miller, Classical Quantum Gravity **30**, 145009 (2013).
[133] I. Musco, Phys. Rev. D **100**, 123524 (2019).
[134] A. Escrivà, C. Germani, and R. K. Sheth, Phys. Rev. D **101**, 044022 (2020).
[135] A. Escrivà, C. Germani, and R. K. Sheth, J. Cosmol. Astropart. Phys. 01 (2021) 030.
[136] I. Musco, V. De Luca, G. Franciolini, and A. Riotto, Phys. Rev. D **103**, 063538 (2021).
[137] Y. Inoue and A. Kusenko, J. Cosmol. Astropart. Phys. 10 (2017) 034.
[138] P. Montero-Camacho, X. Fang, G. Vasquez, M. Silva, and C. M. Hirata, J. Cosmol. Astropart. Phys. 08 (2019) 031.
[139] A. Katz, J. Kopp, S. Sibiryakov, and W. Xue, J. Cosmol. Astropart. Phys. 12 (2018) 005.
[140] V. Poulin, P. D. Serpico, F. Calore, S. Clesse, and K. Kohri, Phys. Rev. D **96**, 083524 (2017).

[141] F. Capela, M. Pshirkov, and P. Tinyakov, Phys. Rev. D **87**, 123524 (2013).
[142] H. Niikura, M. Takada, N. Yasuda, R. H. Lupton, T. Sumi, S. More, T. Kurita, S. Sugiyama, A. More, M. Oguri *et al.*, Nat. Astron. **3**, 524 (2019).
[143] L. Wyrzykowski, J. Skowron, S. Kozlowski, A. Udalski, M. K. Szymanski, M. Kubiak, G. Pietrzynski, I. Soszynski, O. Szewczyk, K. Ulaczyk *et al.*, Mon. Not. R. Astron. Soc. **416**, 2949 (2011).
[144] K. Griest, A. M. Cieplak, and M. J. Lehner, Phys. Rev. Lett. **111**, 181302 (2013).
[145] P. Tisserand *et al.* (EROS-2 Collaboration), Astron. Astrophys. **469**, 387 (2007).
[146] Y. Ali-Haïmoud and M. Kamionkowski, Phys. Rev. D **95**, 043534 (2017).
[147] D. Gaggero, G. Bertone, F. Calore, R. M. T. Connors, M. Lovell, S. Markoff, and E. Storm, Phys. Rev. Lett. **118**, 241101 (2017).
[148] B. Carr, K. Kohri, Y. Sendouda, and J. Yokoyama, Rep. Prog. Phys. **84**, 116902 (2021).
[149] A. M. Green and B. J. Kavanagh, J. Phys. G **48**, 043001 (2021).